Presented at 1994 conference on Advanced Earth to Orbit Propulsion Technology

SSME PARAMETER ESTIMATION AND MODEL VALIDITY USING RADIAL BASIS FUNCTION NEURAL NETWORKS

Claudia M. Meyer[1], William A. Maul[1], and Atam P. Dhawan[2]

[1]NYMA, Inc.
2001 Aerospace Parkway
Brook Park, OH 44142
[2]Department of Electrical and Computer Engineering
University of Cincinnati
Cincinnati, OH 45221

Abstract

Sensor validation is a primary component of the real-time and post-test health management systems being developed for rocket engines. Analytical redundancy models are being used to estimate critical parameters. These estimates, when compared to sensed values, provide information on the health of the sensors. Complex models are required to describe highly nonlinear systems. In addition, quantitative information on the validity of the model inputs is needed to differentiate between input and output sensor failures in the event of large deviations between the actual and model predicted values. The model input validity information provides confidence in the use of the model estimates for health monitoring decisions. Radial Basis Function Neural Networks (RBFNNs) are well-suited for nonlinear function approximation. Furthermore, internal network parameters and the training data used to compute these parameters can be used to indicate the validity of the model inputs. The prediction and model input validity capabilities of RBFNNs were demonstrated on Space Shuttle Main Engine parameters during the highly nonlinear startup transient. RBFNNs were used to model the Oxidizer Preburner chamber pressure, a parameter which has no hardware redundancy, and the High Pressure Oxidizer Turbine discharge temperature, a redlined parameter. Good prediction accuracy was achieved over a large number of test firings. The model input validity indicators responded to simulated hard and soft input sensor failures and correctly identified the failed input parameters.

I. Introduction

Rocket engine system reliability could be improved by systems which validate all sensors used for control, redline limit monitoring and advanced anomaly detection.[1,2] Current efforts to develop an automated sensor validation system for the Space Shuttle Main Engine (SSME) is based on analytical redundancy techniques in which actual sensor data are compared with model-predicted values. Bayesian probability theory is used to combine the information from a network of sensors and models into a single solution describing the health of each sensor under consideration. The models used consisted of first and third order binary empirical correlations which can adequately approximate a large number of parameters during mainstage operation of the SSME. However, more complex models, such as neural networks, are required during the highly nonlinear startup transient.[1]

Multiple input regression techniques and feedforward neural networks trained with the backpropagation algorithm have been used to approximate parameters during the highly nonlinear startup transient.[1-3] Good prediction accuracy has been achieved, but these techniques do not provide an estimate of the validity of the model inputs. Therefore, a deviation between actual and predicted values could be due to a model input sensor failure or a sensor failure of the parameter being modeled. Radial Basis Function Neural Networks (RBFNNs) are well-suited for nonlinear function approximation,[4] and have internal network parameters which can be directly used as indicators of input validity.[5] For example, large prediction error accompanied by high input validity indicates that the output sensor has failed. In this case, the predicted value can be used for continued process monitoring. In addition, RBFNNs are faster and easier to train than feedforward neural networks trained with backpropagation and are not prone to getting stuck in local minima.[5-7]

In this investigation, RBFNNs were used to model the Oxidizer Preburner (OPB) chamber pressure, a parameter which does not have hardware redundancy, and the High Pressure Oxidizer Turbine (HPOT) discharge temperature, a redlined parameter, during the SSME startup transient. The training set consisted of data from the first six seconds of eight nominal test firings. The trained models were validated using data from twenty-seven nominal test firings. Data for all thirty-five test firings were collected on the same test stand. An SSME configuration consists of

several line replaceable units, including low pressure and high pressure fuel and oxidizer turbopumps, a main combustion chamber, a nozzle and a controller. These thirty-five training and validation test firings represent a large number of combinations of line replaceable units; because SSME components are frequently interchanged, models which are insensitive to hardware substitutions are desired.

The prediction performance on the training and validation test firings was measured by the Normalized Root Mean Square (NRMS) error. Simulated drifts and hard sensor failures were injected into the nominal test firings. Scenarios involving one and two input sensor failures were considered. Two types of model input validity indicators were used to quantify the validity of the inputs used to generate the prediction and to isolate one or more failed inputs. The input validity information can be provided to the health management system in order to increase the confidence and reliability of decisions made based on the model output. High validity indicates that the prediction can be used to make health monitoring decisions. Low validity indicates that the information used to make the prediction is invalid due to an input sensor failure, or possibly an engine anomaly. In this case, large deviations between actual and predicted values are not due to a sensor failure in the parameter being modeled. Models developed using RBFNNs could be used to provide startup sensor validation capability to the system currently under development.[1]

II. RBFNN Background

RBFNNs have been shown to be universal function approximators.[7,8] RBFNN theory is extensively described in the literature.[4-8] The specific implementation used in this investigation is summarized below.

As shown in Figure 1, RBFNNs consist of a input layer for distribution of the input vector, a single hidden layer of processing units (basis functions) and an output summation unit. The connections between the hidden and output layers are weighted. An input vector $\boldsymbol{x}$ with components 1 to n is presented to each processing unit. A processing unit has a centroid vector $\boldsymbol{c}_i$ which determines the location of the center of the radial basis function and a variance σ_i^2 which determines the width of the function. The radial basis function, ϕ, used in this investigation is Gaussian and is applied to the Euclidean distance as follows:

$$\phi(\boldsymbol{x}, i) = \exp\left(-\frac{\|\boldsymbol{x}-\boldsymbol{c}_i\|}{2\sigma_i^2}\right) \qquad (1)$$

The output of each unit is then weighted and summed by the output summation unit to obtain the network output or prediction. The weights are determined using matrix inversion techniques.[9]

In addition to the weights, the RBFNN parameters which need to be established are the number of centroids, and their locations and variances. The locations and widths of the radial basis functions depend on the data being presented to the network. A variety of algorithms can be used including k-means clustering and learning vector quantization. A single-pass clustering algorithm was used in this investigation.[10] When applying this algorithm, all patterns are first randomized. The first vector is then assigned to a cluster. All other vectors are sequentially examined to see if they fall within a predetermined distance threshold of the cluster center. The cluster center is recomputed each time a vector is assigned to it. Once all vectors have been examined for the current cluster, the first vector which has not been assigned becomes the next cluster center. Processing continues until all vectors have been assigned. With single-pass clustering, the number of centroids is not predetermined. Finally, cluster variances are computed from the data using a neighborhood of p-nearest centroids of surrounding clusters.[7] The variance of a centroid is taken to be the mean of the square Euclidean distance from the centroid of that cluster to the p-nearest centroids. This method of computing variances helps to improve the interpolation capability of the RBFNN and the smoothness of the fitted function.

The prediction performance of the trained network was assessed by computing the NRMS error, which is calculated as follows:

$$NRMS = \sqrt{\frac{\sum_{i=1}^{m} (y_i - \hat{y}_i)^2}{\sum_{i=1}^{m} y_i^2}} \qquad (2)$$

where $\hat{y}_i$ is the predicted value, y_i is the actual value, and m is the number of time slices in the start profile. The NRMS error is indicative of the overall average accuracy of the prediction.

III. Model Input Validity Indicators

Model input validity indicators can be extracted from internal RBFNN parameters and from the training data used to compute these parameters in a straightforward manner. Two types of model input validity indicators are considered. These are the maximum centroid activation and the confidence values. The maximum centroid activation is determined from the activations of the centroids which are automatically computed when the RBFNN is used for prediction. The confidence values are based directly on the populations used to determine the centroids.

When an input is applied to the trained RBFNN, each centroid produces an output or *activation*. Since each centroid was determined from a portion of the training data, the activation indicates how close the input vector is to the training data represented by that centroid. Two factors combine to generate the activation: the distance between the input vector and the centroid, and the centroid variance. A low activation for a given node indicates that the input vector is not close to the training data used to establish that centroid. A high activation indicates that the input vector is similar to the training data represented by that centroid. If all centroids have low activations for a given input vector, then that input vector is not close to any of the training data, and the value predicted by the model is an extrapolation. If at least one activation is high, then the given input vector falls within the realm of experience of the network and the output does not represent an extrapolation. Therefore, the maximum centroid activation over all centroids provides a good indication of the usefulness of the output produced by the current input vector.[5] Figure 2(a) shows the centroid activations for an input vector when all of the individual inputs are nominal, and Figure 2(b) shows the centroid activations when one input has been failed. There are 49 centroids in the example shown. As can be seen, there are no large activations in the event of an input sensor failure. The Gaussian radial basis function (Eq. 1) ensures that all activations fall in the interval (0,1]. The maximum centroid activation assigned to the input vector in Figure 2(a) is close to one, while the maximum centroid activation assigned to the input vector in Figure 2(b) is just slightly greater than zero.

The confidence values rely on the computation of the actual standard deviation of a centroid in all dimensions, and therefore provide information to isolate faulty inputs. To justify this statistical computation, all centroids which have a population smaller than four are discarded. For all remaining centroids, the standard deviation in each dimension is computed from that centroid's population. A generic fuzzy membership function is established to indicate if an incoming vector belongs to a given population. Confidence values are computed for each dimension as follows. If an input is within a certain number of standard deviations of the mean for the dimension, the confidence for that dimension is assigned a value of 1. The value for the specific number of standard deviations represents the 99.5 per cent confidence interval, and varies from centroid to centroid based on the size of the population used to establish the centroid. For example, the number of standard deviations is 3.169 for a centroid with a population of thirty and 2.854 for a centroid with a population of twenty.[11] The confidence value gradually decreases from one at the number of standard deviations represented by the 99.5 per cent confidence interval to zero at twice that number of standard deviations. When an unknown input vector is presented to the RBFNN, confidence values for each centroid are examined to identify centroids with high confidence values in all dimensions. The total confidence value assigned to a centroid for a given input vector is the sum of the individual dimensional confidence values. The maximum total confidence observed over all centroids is the total confidence value assigned to the current input vector. Since several centroids may have identical total confidence values, the set of confidence values of the centroid which has the largest minimum dimensional confidence value is selected for the current input vector. For example, in an RBFNN with four inputs, [.6, .6, 1, 1] and [.4, .8, 1, 1] both have a total confidence of 3.2. The first set of confidence values would be selected for the current input vector because the second set contains a smaller individual dimensional confidence than the first set.

The confidence values can be displayed in a variety of ways. The information provided by the total confidence is similar to that provided by the maximum centroid activation; it provides an overall assessment of the closeness of the input vector to the training data used to establish the centroids. The individual confidence values for each dimension provide information as to which inputs are causing a low total confidence. With individual confidence values, one can distinguish between small decreases in confidence for several input parameters and a large decrease in confidence for one input. This capability may prove useful in the detection of engine failures other than sensor failures.

IV. Application to SSME Data

The methodology presented in this paper could be used to model any SSME or other system parameter which has sufficient analytical redundancy in the available instrumentation suite. Sufficient analytical redundancy can be described in terms of modeling error acceptable to the user. Two SSME parameters were selected in this investigation: the OPB chamber pressure, a parameter which has no hardware redundancy, and the HPOT discharge temperature, a redlined parameter. These parameters are both on the oxidizer side of the SSME which is more sparsely instrumented than the fuel side. The HPOT discharge temperature experiences very large nominal test-to-test variability, while the OPB chamber pressure is more repeatable from test-to-test. Several issues were addressed in the application of RBFNNs to SSME data. These include the selection of model inputs, the selection of training and validation test firings, the determination of an appropriate distance threshold for the single-pass clustering algorithm, and the simulation of input sensor failures.

The engine measurements in the model input vector were chosen because of their physical interdependence with the parameter being modeled. Four inputs were selected for

the OPB chamber pressure and five inputs were selected for the HPOT discharge temperature; the parameters are given in Table 1. Prior to presentation to the RBFNN training algorithm, all inputs and the output were normalized to fall within the range [-0.5 0.5]. The minimum and maximum values used for normalization were determined from all training and validation test firings.

A total of thirty-five test firings was used to train and validate the RBFNN models. In order to provide the networks with sufficient examples of the range of nominal behavior experienced by the SSME, eight test firings were used for training. The test firings selected for training were B1050, B1055, B1056, B1070, B1073, B1079, B1081, and B1084. B1 indicates the test stand at Stennis Space Center on which the firings were conducted, and the last three digits indicate the test firing number. These firings represent the range of nominal behavior experienced by the inputs and outputs listed in Table 1. The twenty-seven test firings used for validation consisted of all test firings between B1049 and B1086, inclusive, which were not used for training and which had a complete six-second start transient.

The training test firings were used to generate training vectors for the RBFNNs; these training vectors were used for data clustering and RBFNN weight determination. Data from 0.0 to 5.96 seconds were used; the SSME sampling interval of 40 msec resulted in 149 patterns per test firing. Eight training test firings generated 1192 initial training patterns. Prior to determination of the RBFNN weights, the single-pass clustering algorithm was applied to the training patterns to compute the cluster center locations. As indicated in the previous section, cluster centers with a population less than four were discarded. The threshold distance used in the single-pass clustering algorithm was adjusted until 90 per cent or more of the vectors from each test firing contributed to the final cluster centers. The distance values were dependent on the parameter being modeled and were determined by trial and error. In each case, a smaller threshold than the one selected resulted in too many vectors being discarded, and a larger threshold resulted in too few cluster centers.

After training, The NRMS error was computed for all training and validation test firings. In addition, the maximum centroid activation, the individual dimensional confidence values, and the total confidence were determined for the training and validation test firings. None of these test firings contained input or output sensor failures. Examples of model input validity for nominal test firings provided a baseline for comparison with model input validity indicators in the presence of input sensor failures.

Various input sensor failure scenarios were constructed to illustrate the utility of the model input validity indicators. Hard sensor failures were simulated by freezing a sensor value at the sensor failure initiation time; the sensor value remained constant for the remainder of the start profile. Soft sensor failures were simulated by injecting a drift of constant magnitude into an input parameter at the sensor failure initiation time. Figures 3(a) and 3(b) show examples of simulated hard and drift sensor failures of the Preburner Boost Pump (PBP) discharge pressure on validation test firing B1067. Both single and multiple input sensor failures were considered. The case numbers, along with the model used, the failed input sensor(s), and the sensor failure type and initiation time are presented in Table 2. Cases 1-3 explore the impact of single input sensor failures. Case 4 considers two input sensor failures.

V. Results and Discussion

Data from eight nominal test firings were used to train RBFNNs to model two parameters, the OPB chamber pressure and the HPOT discharge temperature, during the SSME startup transient. The performance of the trained networks was assessed using twenty-seven validation firings. Nominal inputs and simulated input sensor failures were considered. All nominal and simulated input sensor failure examples depicted are from validation firing B1067.

The single-pass clustering algorithm generated the centroids used by the RBFNNs. All centroids were computed from a population of at least four training patterns. The distance thresholds selected for use in the single-pass clustering algorithm resulted in 49 centroids for the OPB chamber pressure model and 40 centroids for the HPOT discharge temperature model. The centroids formed by the single-pass clustering, together with the variances and weights between the hidden and output units, give the RBFNN its prediction capability.

The NRMS errors computed for the training and validation test firings indicate that each model provides good prediction of the specified parameter over the entire startup profile and for a variety of engine configurations. The OPB chamber pressure model NRMS errors ranged from .003 to .017 on the validation test firings, with a mean value of .0094. The HPOT discharge temperature model NRMS errors ranged from .011 to .063 on the validation test firings, with a mean of .028. The OPB chamber pressure model performed better than the HPOT discharge temperature model on the training and validation firings. This can be attributed to several factors. The HPOT discharge temperature exhibits more nominal variability during the six second start transient than the OPB chamber pressure. This variability is only partially accounted for by the model input set. Due to the harsh environment on the oxidizer side of the SSME, additional sensor information,

such as the high pressure oxidizer pump shaft speed, is not available. Furthermore, temperature sensors are much slower to respond than pressure and shaft speed sensors, making sensor dynamics an important component of the modeling process. An example of the prediction capability for both models is presented in Figures 4(a) and 4(b) for validation test firing B1067; actual and RBFNN predicted values are shown. These figures are representative of the performance of the two models on the nominal validation firings. NRMS errors for the OPB chamber pressure and HPOT discharge temperature models for test B1067 were .009 and .028, respectively.

In addition to the prediction capability of the RBFNNs, internal network parameters and information used to derive these parameters were used to validate the inputs being presented to the network. Figures 5 and 6 show the maximum centroid activation and the total confidence indicator for the OPB chamber pressure and HPOT discharge temperature models on nominal test firing, B1067. Figures 5(a) and 6(a) show the maximum centroid activations as a function of time. Because the centroids established by the single-pass clustering algorithm are well-distributed over the startup profile, the values for maximum activation are high (> 0.75) for all thirty-five nominal firings throughout the start transient. Figures 5(b) and 6(b) show the total confidence value for the input vectors presented to the RBFNN; the upper limit on the total confidence is a multiple of the number of input values. The total confidence indicates how consistent the entire input vector is with the experience base encoded by the model, and is high throughout the start transient for all thirty-five nominal test firings.

The maximum centroid activation and confidence metrics provided clear sensor failure indications when tested against the scenarios listed in Table 2. In case 1, a hard failure of the Preburner Boost Pump (PBP) discharge pressure was introduced at 3.0 seconds. Figures 7(a) and 7(b) show the increase in error between the RBFNN predicted and the actual sensed values for the OPB chamber pressure. Figures 8(a) and 8(b) show a dropoff in maximum centroid activation and in the total confidence. This indicates that the input vectors encountered after 3.0 seconds are invalid. As can be seen, both of these metrics provide similar information on the overall validity of the input vectors. Furthermore, an examination of the individual confidence values identifies the PBP discharge pressure as the failed input parameter. Thus, the model input validity indicators show that the deviation between actual and predicted values is not due to a sensor failure of the parameter being modeled. Upon isolation, the failed PBP discharge pressure reading would no longer be used to make health monitoring decisions. Use of the OPB chamber pressure RBFNN model could continue if a redundant channel or synthesized value were available to replace the failed input sensor reading.

The RBFNN model input validity indicators were also applied to an input failure in the HPOT discharge temperature model. Sensor failure case 2 investigated the impact of a hard sensor failure of the OPB chamber pressure on the HPOT discharge temperature model. The response of the RBFNN prediction and the model input validity indicators were similar to those experienced in case 1. The OPB chamber pressure was disqualified shortly after the initiation of the sensor failure.

Sensor failure case 3 examined a drift in the Fuel Preburner (FPB) chamber pressure for the OPB chamber pressure model. Since the amount of time within the start profile is less than six seconds, the drift condition used was large, 100 psia/second, and was initiated early in the start profile, start+1.0 seconds. Small drifts or drifts occurring late in the start profile would not exhibit much effect on the prediction of the RBFNN and may not deviate significantly from the experience base used to construct the models. For the drift considered, a dropoff in all model input validity indicators was observed, but the dropoff was more gradual due to the nature of the input sensor failure. The increase in the deviation between the actual and predicted values for the modeled parameter could therefore be attributed to an input sensor failure. The individual confidence value for the FPB chamber pressure fell to zero, thus correctly identifying this parameter as the failed input.

Finally, sensor failure case 4 considered multiple input sensor failures. This case combines a drift and a hard failure. Prediction errors are similar to those observed in case 1. Figures 9(a) and 9(b) illustrate that the model input vectors become invalid shortly after 3.0 seconds. Figures 10(a) - 10(d) show the individual confidence values. The input numbers one through four refer to the model inputs in the order in which they are listed in Table 1. Soon after initiating the hard failure of the PBP discharge temperature, Figure 10(c) indicates zero confidence in this parameter. Furthermore, as the deviation between the actual and simulated input sensor failure values for the drifting FPB chamber pressure increase, the confidence for the FPB chamber pressure deteriorates. Monitoring of individual confidence values can be used to detect and isolate multiple sensor failures. Due to the small number of inputs, however, it may be difficult to distinguish between multiple input sensor failures and engine anomalies. The nature and timing of the multiple sensor failures can also affect the ability of the network to correctly identify the failed instrumentation. If, for example, two of four inputs were to fail hard (i.e., freeze at their current values) at exactly the same time, the network would not conclusively identify the correct two sensors as failed since both pairs of inputs are within the experience base of the network. The model input validity indicators, maximum centroid activation and total confidence, would clearly indicate, however, that the combination of inputs is invalid.

The model input validity indicator appropriate for a given application depends on the information required and on computing considerations. The centroid activations are computed automatically in generating the RBFNN prediction. The maximum of these values for a given input vector is a good indicator of the overall validity of the input vector. Since a low maximum centroid activation indicates that one or several of the individual inputs used to generate the predicted value are not valid, the output of the RBFNN model should not be used for decision-making. The total confidence provides a similar indication of overall input validity as the maximum centroid activation. Furthermore, in the case of single and some multiple input sensor failures, the individual confidence values provide a clear indication of which input sensor has failed. Since the confidence values are based on the populations used to compute the centroids and not on values used directly for the RBFNN prediction, however, their use represents additional computational overhead.

VI. Concluding Remarks

Radial Basis Function Neural Networks (RBFNNs) have been used to efficiently and accurately model parameters responding to highly nonlinear conditions. Although traditional neural network and regression techniques can provide similar prediction capabilities, they do not provide an estimate of the validity of the inputs used to make the prediction. SSME data were used to demonstrate the ability of the RBFNNs to predict critical parameters and to quantify the validity of the model inputs. Two types of model input validity indicators, the maximum centroid activation and the confidence values, provided clear indications that one or more input sensor failures had occurred by recognizing inconsistent relationships among highly correlated input parameters. In addition, the individual confidence values correctly identified which inputs had failed.

The model validity indicators provide a quantitative means to determine if the model prediction should be used to make health monitoring decisions. A large deviation between actual and model predicted values accompanied by high model input validity is indicative of a sensor failure in the parameter being modeled. Therefore, this sensor should not be used for control, redline limit monitoring or advanced anomaly detection. A redundant channel or the RBFNN predicted value can be used in place of the failed sensor value. A large deviation between actual and model predicted values accompanied by low model input validity indicates an input sensor failure. Use of the RBFNN model output could continue if a redundant channel or synthesized value were available to replace the failed input sensor reading.

The prediction and model input validity capabilities of RBFNNs can be used as part of an overall sensor validation system. Such a system will enhance rocket engine safety and reliability by ensuring that all sensors used to make control, redline limit monitoring and advanced anomaly detection decisions have been validated.

Acknowledgements

This work was supported by OACT out of NASA Lewis Research Center under contract NAS3-27186 and cooperative agreement NCC3-308.

References

1. Bickmore, T., "Real-Time Sensor Data Validation", NASA CR-195295, March, 1993.
2. Hawman, M.W.; Ruiz, C.A., and Galinaitis, W.S., "Space Shuttle Main Engine Health Monitoring System", NASA CR-195328, April, 1994.
3. Meyer, C.M. and Maul, W.A., "The Application of Neural Networks to the SSME Startup Transient", AIAA Paper 91-2530, June 1991.
4. Park, J. and Sandberg, I.W., "Universal Approximation Using Radial-Basis-Function Networks", Neural Computation, **3**(1), pp. 246-257, 1991.
5. Leonard, J.A., Kramer, M.A., and Ungar, L.H., "A Neural Network Architecture That Computes Its Own Reliability", Computers in Chemical Engineering, **16**(9), pp. 819-835, 1992.
6. Wheeler, K.W.; Dhawan, A.P. and Meyer, C.M.,"SSME Sensor Modeling Using Radial Basis Function Neural Networks", *AIAA Journal of Spacecraft and Rockets*, in press, 1994.
7. Moody, J. and Darken, C.J., "Fast Learning in Networks of Locally-Tuned Processing Units", Neural Computation, **1**, pp. 281-294, 1989.
8. Powell, M.J.D., "Radial Basis Functions for Multivariable Interpolation: A Review", in *Algorithms for Approximation* (Mason, J.C. and Cox, M.G., eds.), Clarendon Press, Oxford, 1987, pp. 143-167.
9. Press, W.H.; Teukolsky, S.A.; Vetterling, W.T., and Flannery, B.P. *Numerical Recipes in C - The Art of Scientific Computing, 2nd Edition.* Cambridge University Press, Cambridge, 1992, pp. 32-70.
10. Dhawan, A.P.; Wheeler, K.R., and Doniere, T.F.,"SSME Parameter Modeling with Neural Networks", 1994 Aerospace Atlantic Conference, April 18-22, 1994.
11. DeGroot, M.H. *Probability and Statistics.* Addison-Wesley Publishing Company, pp. 692-3.

input \ model	HPOT Discharge Temperature	OPB Chamber Pressure
OPOV Position	x	x
FPB Chamber Pressure	x	x
PBP Discharge Pressure		x
MCC Pressure		x
PBP Discharge Temperature	x	
OPB Chamber Pressure	x	
LPOP Shaft Speed	x	

Table 1. Parameters that are inputs for the OPB chamber pressure and HPOT discharge temperature RBFNN models.

Case	Model	Input Failed	Failure Type	Start Time
1	OPB Chamber Pressure	PBP Discharge Pressure	hard	3.0 secs
2	HPOT Discharge Temp	OPB Chamber Pressure	hard	3.0 secs
3	OPB Chamber Pressure	FPB Chamber Pressure	100 psia/sec drift	1.0 secs
4	OPB Chamber Pressure	FPB Chamber Pressure PBP Discharge Pressure	50 psia/sec drift hard	1.0 secs 3.0 secs

Table 2. RBFNN input sensor failure cases for the OPB chamber pressure and HPOT discharge temperature RBFNN models.

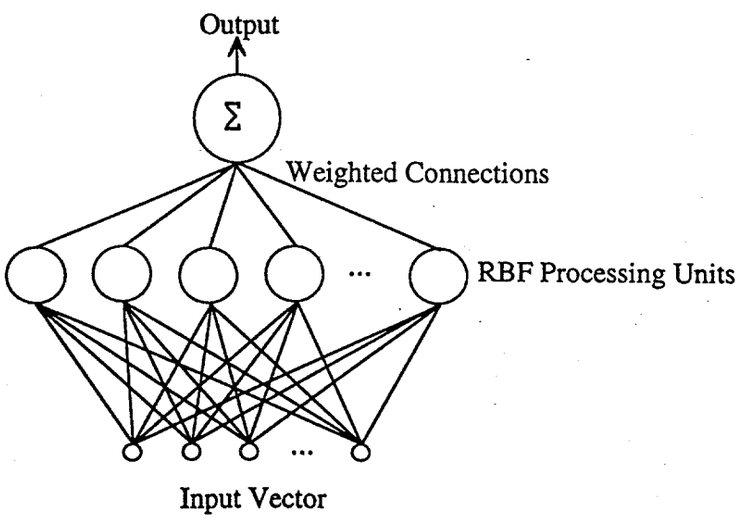

Figure 1. Radial Basis Function Neural Network

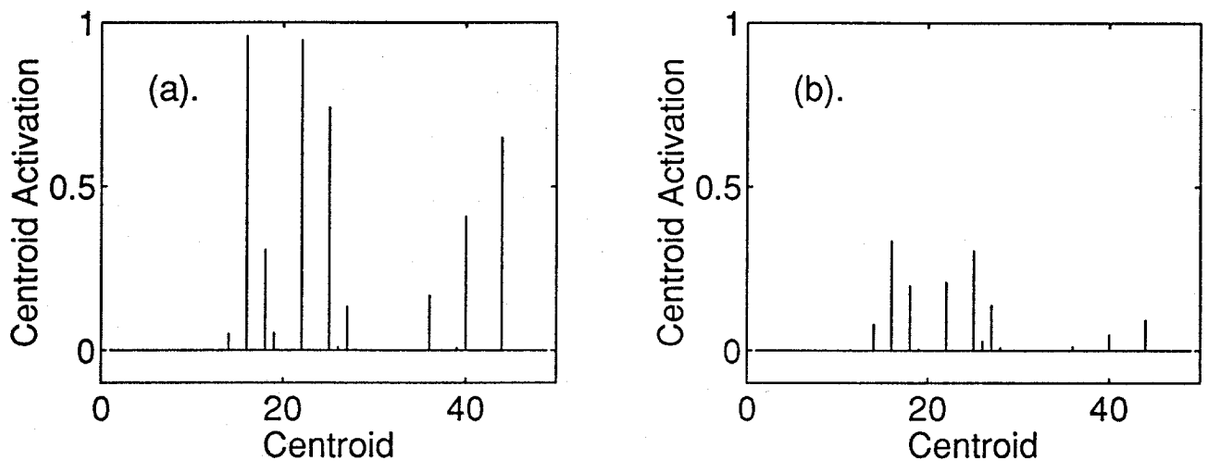

Figure 2. The centroid activation values for each centroid at time start + 3.8 seconds for test firing B1067 with (a). all nominal input values and (b). with a single sensor failure.

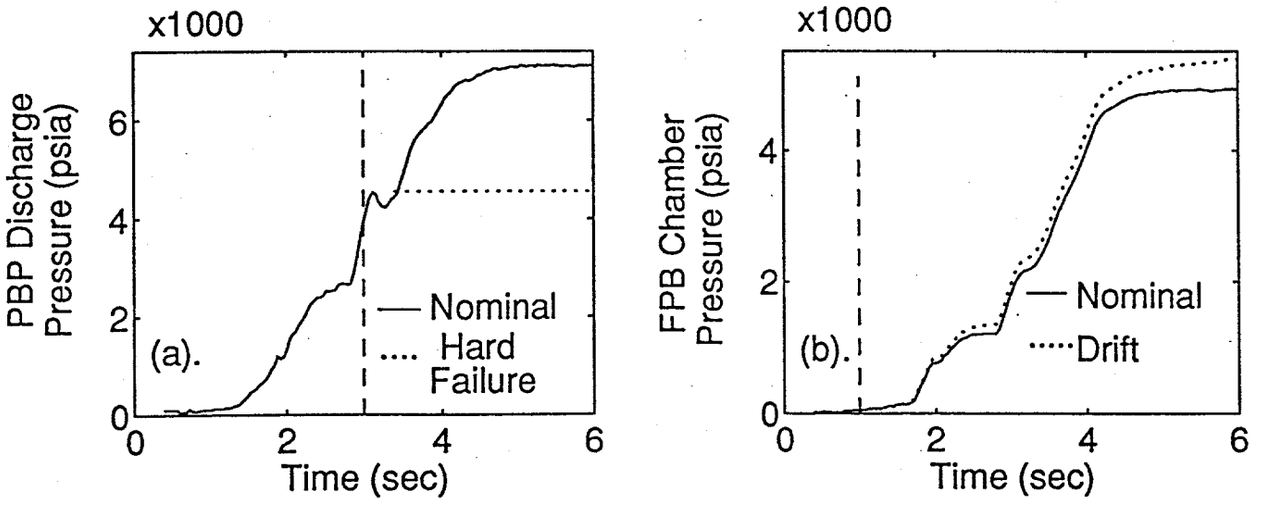

Figure 3. Examples of input sensor failures: (a). hard failure of the PBP discharge pressure and (b). drift failure of the PBP chamber pressure.

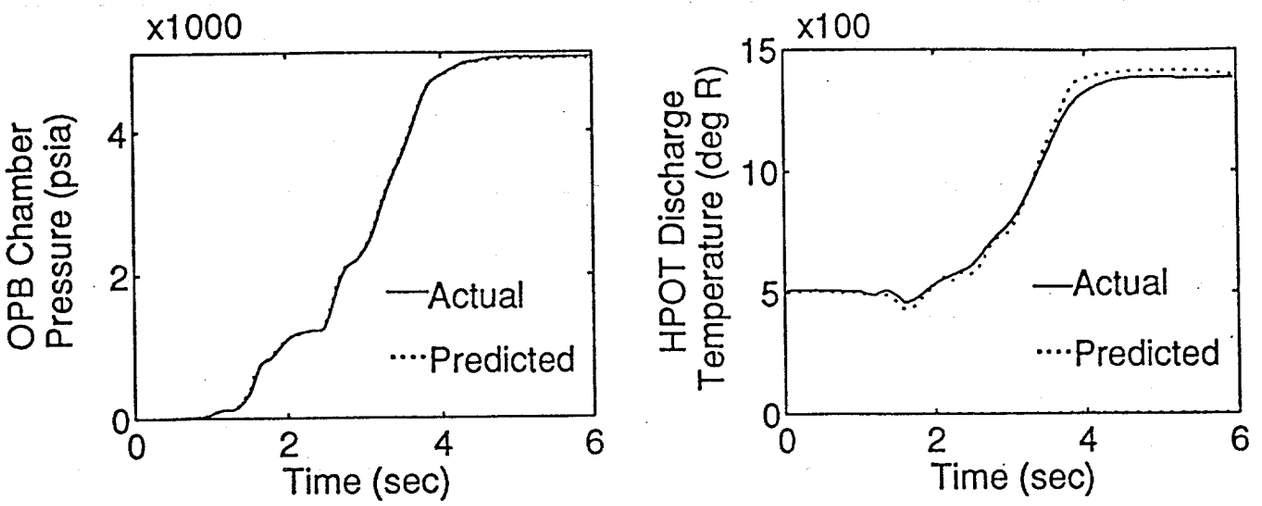

Figure 4. The actual and predicted values for (a). the OPB chamber pressure RBFNN model and (b). the HPOT discharge temperature RBFNN model.

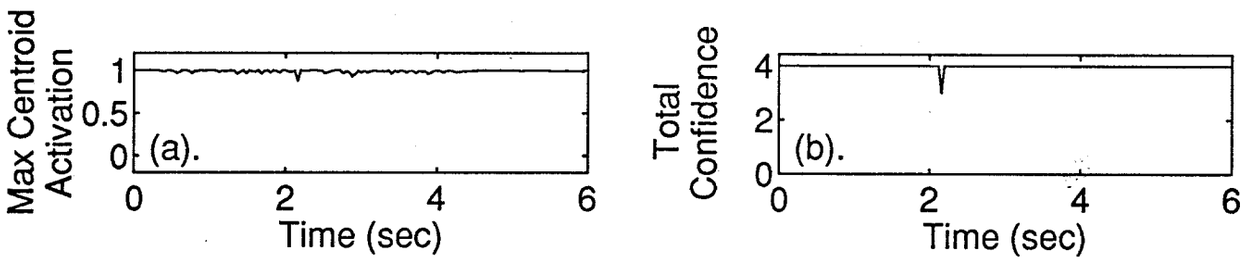

Figure 5. Response of the model validity indicators: (a). the maximum centroid activations and (b). the total confidence values, for the OPB chamber pressure model on validation firing B1067.

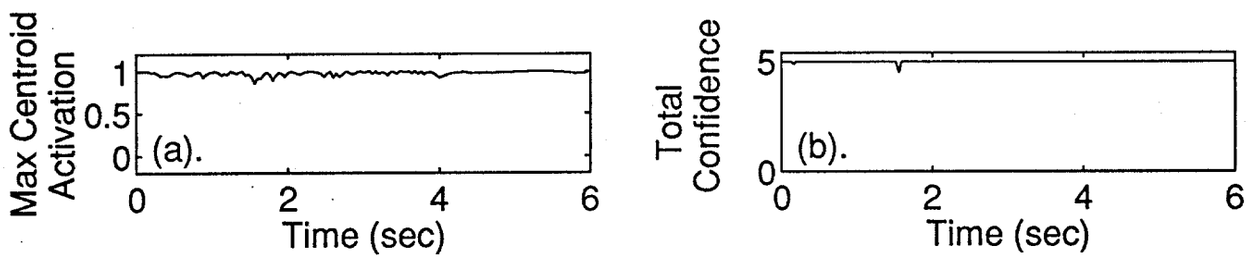

Figure 6. Response of the model validity indicators: (a). the maximum centroid activations and (b). the total confidence values, for the HPOT discharge temperature model on validation firing B1067.

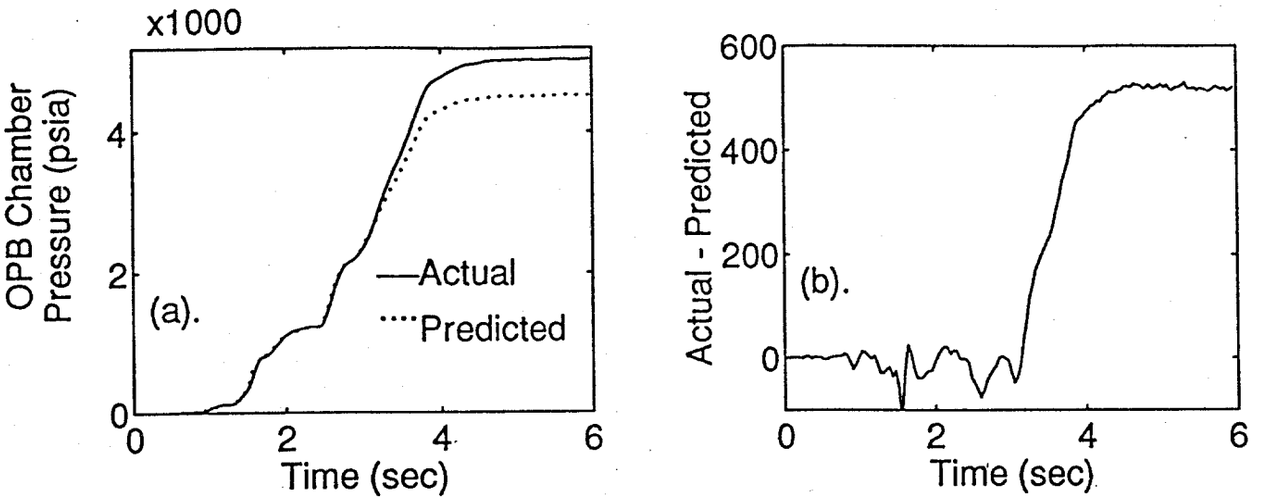

Figure 7. Performance of OPB chamber pressure RBFNN model in the presence of a hard input sensor failure for validation firing B1067: (a). actual and predicted values and (b). the difference between actual and predicted values.

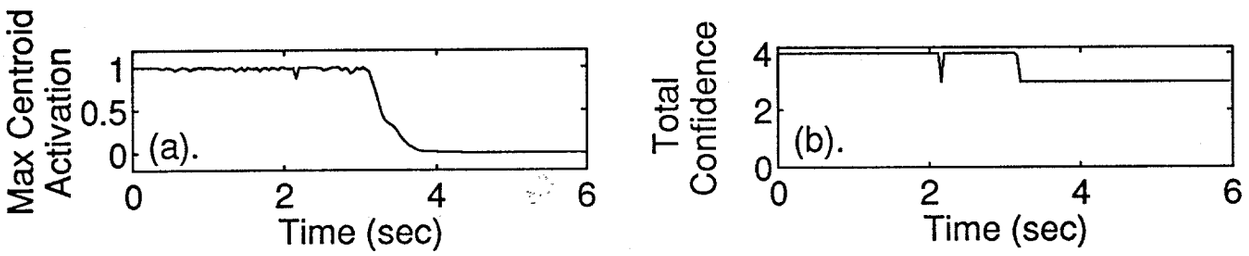

Figure 8. Response of model validity indicators to an input sensor failure in the OPB pressure RBFNN model: (a). the maximum centroid activations and (b). the total confidence values.

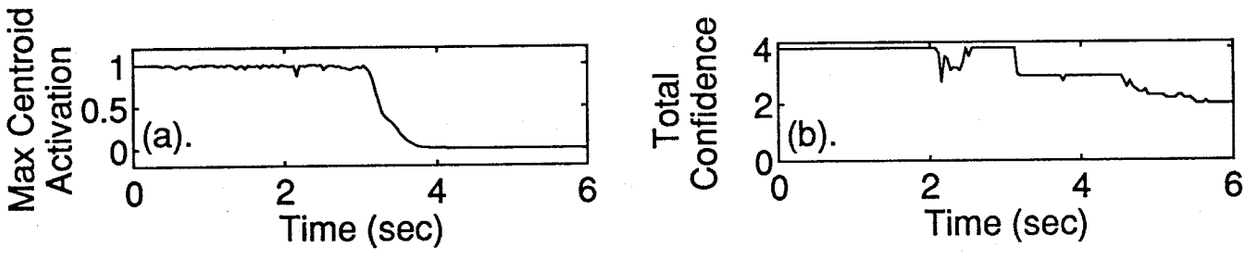

Figure 9. Response of model validity indicators to two input sensor failures in the OPB chamber pressure RBFNN model: (a). the maximum centroid activations and (b). the total confidence values.

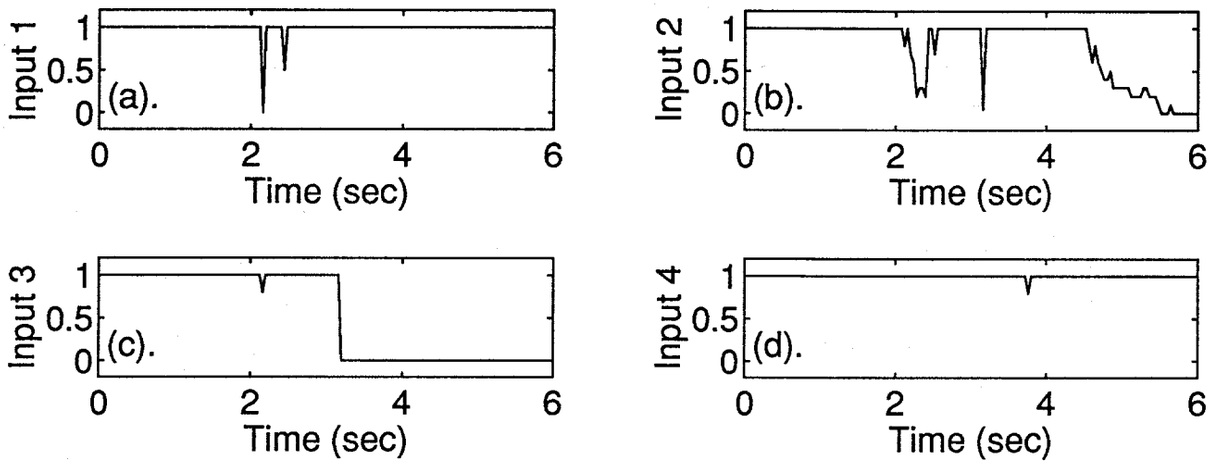

Figure 10. Individual dimensional confidence values for (a). input 1, (b). input 2, (c). input 3 and (d). input 4 of the OPB chamber pressure RBFNN model. Inputs 2 and 3 contained the simulated sensor failures.